CONTROL OF BACTERIAL BIOFILMS BY MICROPARTICLE SPACERS

A Thesis
Presented to
The Academic Faculty

by

Olivia Sergent

In Partial Fulfillment
of the Requirements for the Degree
Bachelor's in Science in the
School of Biomedical Engineering

Georgia Institute of Technology
May 2019

CONTROL OF BACTERIAL BIOFILMS BY MICROPARTICLE SPACERS

Approved by:

Dr. Kyle Allison, Advisor
School of Biomedical Engineering
Georgia Institute of Technology

Dr. Julia Babensee
School of Biomedical Engineering
Georgia Institute of Technology

Date Approved: May 3, 2019

[To the students of the Georgia Institute of Technology]

ACKNOWLEDGEMENTS

I wish to thank Gabrielle Rusch and Laura Meyer, fellow undergraduate researchers in Dr. Kyle Allison's laboratory, for their aid in developing the microparticle spacer for this thesis. Also, I would like to acknowledge my faculty advisor Dr. Kyle Allison, postdoctoral researcher Dr. Xin Fang, and graduate student Devina Puri for their guidance.

TABLE OF CONTENTS

SUMMARY

Bacteria can be found in two distinct states: planktonic or as part of a sessile biofilm. While planktonic, free-floating bacteria are moderately easy to eradicate with antibiotics, bacteria in biofilms are not. Bacterial biofilms are tightly packed together, making it difficult for antibiotics to pass through the film and eliminate the bacteria; this antibiotic resistance makes it difficult to treat many bacterial infections. To try to decrease the antibiotic resistance of bacterial biofilms, this study utilized a microparticle spacer to create distance between cells in biofilms. The microparticle spacer was made by annealing Dynabead magnetic beads to Cholesterol-containing DNA; the Cholesterol on the spacer could bind to the lipid bilayer of bacteria. The spacer was mixed with various proportions of *Escherichia coli* K-12 wild-type and analyzed with fluorescence microscopy to determine binding affinity between the spacer and bacteria. Binding was quantified both visually and computationally, and the two methods were compared to determine accuracy. The spacers and bacteria showed high levels of binding, with over 84.8% of all spacers bound to bacteria according to the visual method. 13.3% difference was determined between the two methods; therefore, the computational method still needs improved precision and accuracy before it is used consistently. Due to a demonstrated high binding affinity, we hypothesize that this microparticle spacer could successfully add space between bacteria in biofilms.

CHAPTER 1

INTRODUCTION

Bacterial biofilms are formed when free-swimming bacteria attach to a substratum in moist environments.[1] According to the National Institutes of Health, around 80% of bacterial infections in humans involve biofilm-associated microorganisms.[2] Some common biofilm locations in humans include along the gastrointestinal tract and on artificial surfaces located in the body, such as implants.[3] As a biofilm, sessile bacteria have an increased tolerance for antibiotics. The cells in these biofilms are closely packed, which makes it harder for antibiotics to flow through the biofilm and treat bacteria. The insufficient nutrients and space provided to bacteria in biofilms cause the bacteria to grow slowly, increasing resistance. Another reason biofilms are highly resistant to antibiotics is because multiple species of bacteria can grow in one biofilm. Biofilms contain heterogeneous and spatially stratified structures, which allow chemical gradients in the concentration of nutrients to find individual niches for multiple species of bacteria to live together in the same biofilm. The different species of bacteria can transfer resistance genes to the species surrounding them, increasing the overall resistance.[4] Since bacterial biofilms have such a high resistance to antibiotics, there is interest in finding new methods to decrease tolerance levels and eradicate the biofilms. These methods could help eliminate bacterial infections.

Many researchers have analyzed how to disperse or prevent the buildup of bacterial biofilms. One method of dispersal that was discovered was sudden changes in nutrient availability, such as changes in carbon and oxygen levels. Hunt et al found that biofilms under continuous-flow conditions underwent dispersal in response to both sudden decreases and increases in carbon substrate availability.[5] Meanwhile, Applegate and Bryers discovered that oxygen-limited biofilms demonstrated significantly lower shear removal rates and significantly greater biofilm dispersal rates compared to biofilms in oxygen-rich conditions.[6] Other techniques to eradicate these biofilms that have been studied are controlling quorum sensing, implementing surface coatings, and using small molecules and nano-scaffolds.[7,8,9,10] Despite these proposed methods, the efficiency of eliminating the biofilm and decreasing resistance can still be improved.

In contrast to past studies, this study aims to control the biofilm instead of destroy it or prevent its buildup. This new outlook may answer many unknown questions regarding biofilms, as well as find a more effective way to make them less resistant to antibiotics. To control the biofilm, the distance between the bacteria will be regulated. Microparticles of equal size, Dynabeads, will be used as "spacers" that bind to bacteria and create equal separation between the cells. In order for these spacers to stick to the bacteria, an “effector” must be applied to the outside of the microparticles. The "effector" will be made from DNA with a Cholesterol attachment, and it will allow the spacer to attach to the lipid bilayer of the bacteria. This study will contribute to the area of bacteria biofilms by discovering a new, more effective, and highly innovative way to decrease the bacterial persistence of bacterial biofilms.

CHAPTER 2

METHODS AND MATERIALS

For this project, two strands of synthetic DNA (Integrated DNA Technologies) were annealed to each other, and then they were annealed to Dynabead Oligo (dT)25-61002 (ThermoFisher Scientific) microparticles to form the microparticle spacer (see *Figure 1*). One strand of the synthetic DNA, the splint DNA, consisted of a tail of A nucleotides that could bind to the Dynabead's strand of T nucleotides. The other strand, the cholesterol DNA, consisted of a cholesterol attachment, a Texas Red fluorophore, and a strand of nucleotides complementary to the non-A tail of the splint DNA. Complimentary nucleotide sequences between the two strands of DNA and the Dynabead allowed for binding to occur. Agarose slides were created, and the *E. coli* K-12 wild-type bacteria and Bead-DNA complex were added to the slides. The slides were viewed using fluorescence microscopy and analyzed both visually and computationally.

Figure 1. Schematic of microparticle spacer: Dynabead, DNA, and cholesterol attachment.

Annealing the Two Strands of DNA

To anneal the two strands of DNA, a 100 mM solution of cholesterol DNA was made by combining 13 nmol of the cholesterol DNA with 130 µL of nuclease-free water and vortexing on the mixer. The cholesterol DNA solution container was wrapped in aluminum foil in order to protect the red color of the Texas Red fluorophore from decreasing in brightness. A 100 mM solution of splint DNA was also made by combining 11.3 nmol of splint oligo with 113 µL of nuclease-free water and vortexing on the mixer.

Next, 8 μL of the splint solution and 4 μL of the cholesterol solution were placed in a PCR tube. Using a thermocycler, the temperature was set at 80 ℃ for 3 minutes, and then the temperature was decreased by 1 degree/min until 4 ℃ was reached.

Washing the Dynabeads

Before using the Dynabeads for the microparticle spacer, the beads needed to be washed. To wash the beads, 40 μL of beads and 1 mL of DNA annealing buffer (10 mM Tris, pH 7.5-8.0, 50 mM NaCl, and 1 mM EDTA) were placed in a microcentrifuge tube. The microcentrifuge tube was placed on a Dynabead MPC-S magnetic particle concentrator (ThermoFisher Scientific), and the MPC-S separated the beads from the supernatant. The supernatant was removed from the tube, and the beads were resuspended in 40 μL of the DNA annealing buffer. The beads were mixed on a vortex mixer to ensure a homogeneous solution.

Creating the Microparticle Spacer: Annealing Dynabeads to the DNA

To determine the effect of adding an effector to the spacer, two different concentrations of beads to DNA were used. In 2 separate PCR tubes, the mixtures of 10 μL of beads (control without the effector) and 10 μL of beads with an added 2 μL of DNA (spacer with the effector) were created. Using a thermocycler, the mixtures were heated up to 42 ℃ and left for 5 minutes. Then, they were brought back down to 4 degrees at a rate of 1 degree/min. Now, the microparticle spacer had been successfully created.

Making Agarose Slides

To make agarose slides, 5 mL of EZ Rich growth medium was added to a test tube through the usage of a sterilized 25 mL pipette, and then the pipette was properly discarded in a sharps container. Next, 0.1 grams of agarose was properly weighed and added to the test tube. The EZ growth medium and the agarose were mixed to form a 2% agarose solution by placing in a lab oven around 80 ℃ for 20 minutes. After the solution was properly mixed, one sticky side was removed from each of the two microfilms, the

sticky sides were placed together, and small squares the width of the microscope slides were cut out of the microfilms. A circle was cut out of the center of each microfilm square by wrapping a piece of paper around each square and removing the circle with a hole puncher. Then, one of the sticky sides of the square was removed, and the square was placed on center of the microscope slide. The agarose solution was pipetted into the center, hole-punched region of the circle until it overflowed, and a glass cover was quickly placed on top. After letting dry for around 10 minutes, the slide was ready for the bacteria and microparticle spacers to be added.

Combining the Bacteria and the Microparticle Spacer

After making the slides, 1 μL of each of the 2 different bead-DNA mixtures were combined with 10 μL of *E. coli* bacteria in separate test tubes. The test tubes were incubated for 10 minutes, and 2 μL of each of the solutions were added to separate agarose slides. Then, the slides were placed under a Leica inverted microscope for viewing and recording with fluorescence microscopy. For each slide, 100 spacers were imaged and recorded.

Analyzing Microscopy Images Visually

After recording the images, the percentage of microparticle spacers bound to bacteria was analyzed visually. For each image, the number of spacers, which glow red under fluorescence, the number of bacteria, which glow green, and the number of spacers bound to one or more bacteria were counted. The percentage of spacers bound to bacteria was calculated by dividing the number of spacers bound to bacteria by the total number of spacers in the image. Afterwards, a two-sample t-test assuming equal variances with alpha level 0.05 was applied to the two conditions to determine whether they are significantly different.

Analyzing Microscopy Images Computationally

To determine the number of beads bound to bacteria more efficiently, a computational method was generated in MATLAB. This code used image segmentation

procedures to locate and quantify the number of spacers and bacteria in the image based on color. To find the number of spacers, a red threshold was created by separating the image into three separate RGB channels and identifying all the regions of the image that were present in the red channel. When using this same threshold with the original image, only areas of the image with red colorization above this threshold, the same regions that were seen in the red channel, were shown in the image. Therefore, these areas were identified as the spacers. Then, boundaries were found around each spacer and the number of separate spacers was counted. This process was repeated for the bacteria with a green color threshold instead. Afterwards, sub-images were created around each spacer and the number of bacteria in each sub-image was quantified to determine the number of bacteria bound to each spacer. The number of spacers discovered in each image using the computational method was compared to the number of spacers discovered using the visual method by calculating percent difference.

CHAPTER 3

RESULTS

Imaging

After placing the two slides under the microscope, successful images were obtained (see *Figure 2*). For each image, the microparticle spacer fluoresced red, and when the effector was present, a darker ring of red could be seen around the edge of the spacer, showing that the cholesterol successfully bound to the Dynabead. In contrast, the *E. coli* bacteria fluoresced green, and attachment between the spacers and bacteria could be seen.

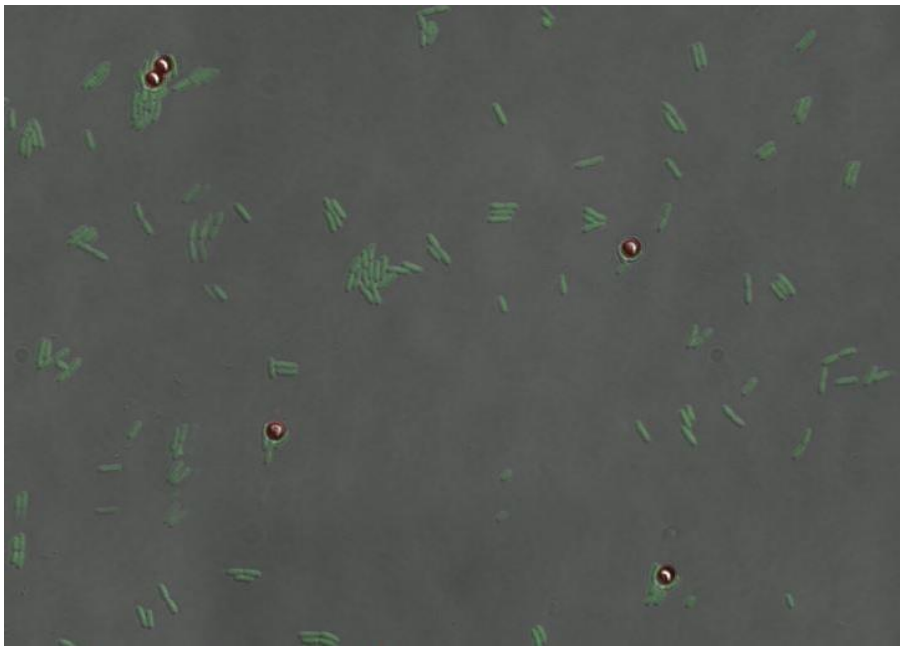

Figure 2. Image of microparticle spacers and bacteria under fluorescence. *The spacers are shown in red while the bacteria are shown in green.*

Data Analysis

Once the number of spacers and bacteria were calculated visually, the average percentage of microparticle spacer binding was found for both conditions. For the microparticle spacers without effector, 2.90% ± 1.85% of the spacers were bound to

bacteria. For the microparticle spacers with effector, 84.8% ± 0.14% of the spacers were bound to bacteria (see *Figure 3*). To test significance, a two-sample t-test with alpha level 0.05 was applied using the two data sets. The two-sample t-test revealed a p-value of 0.000255.

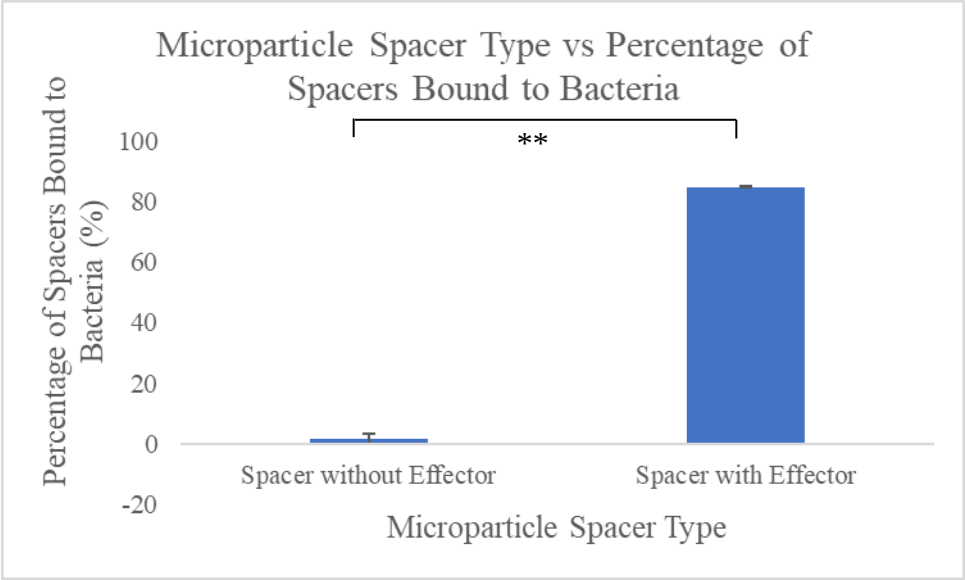

Figure 3. Microparticle Spacer Type vs Percentage of Spacers Bound to Bacteria. *A two-sample t-test revealed a p-value of 0.000255 between the groups, less than the alpha level of 0.05. This small p-value is indicated by the two asterisks between the groups. The error bars represent the standard deviations of the two groups.*

Computational Analysis

When running images through the computational code, red spacers and green bacteria were successfully separated and identified, and boundaries were distinguished around each individual particle (see *Figure 4*). In regions where the spacers were clumped together and too close to identify as individual spacers, the number of spacers in the clump were counted based on the total area of the clump. The area of one spacer was around 2000 pixels, so the total area was divided by 2000 pixels to identify the number of spacers.

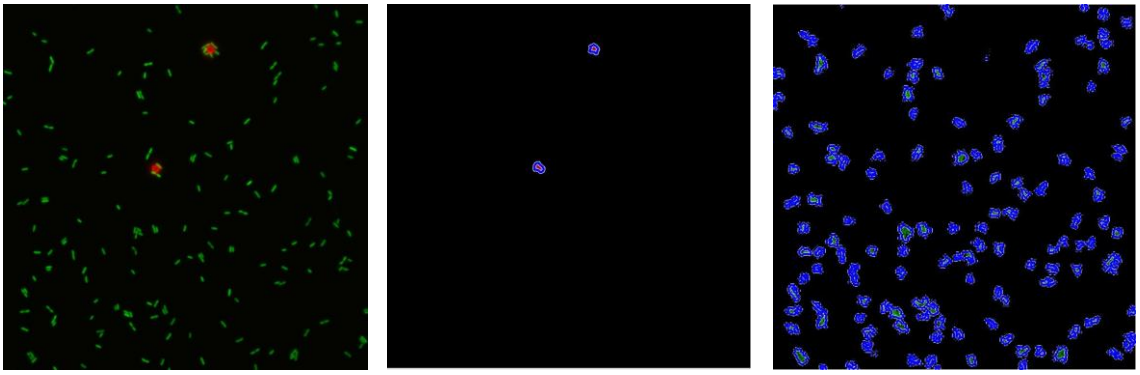

Figure 4. Images of the Bacteria and Spacers Utilized in the Computational Code. *From left to right: a) An image of microparticle spacers and bacteria output from the microscope. b) The same image containing only the red spacers with blue boundaries highlighting the edge of each spacer. c) The same image containing only the green bacteria with blue boundaries highlighting the edge of each bacterium.*

Percent difference between the computational method and the visual method was calculated as 13.3%. Images with lighting issues, such as dark regions where there was not enough oil immersion present, were excluded from this comparison.

CHAPTER 4

DISCUSSION

Statistical Analysis

To determine the significance of the effector, a t-test was performed between the microparticle spacer with effector and the microparticle spacer without effector. The null hypothesis for this test was that the means of the two groups were the same. The t-test revealed a p-value of 0.000255 at a 0.05 confidence interval. Therefore, the null hypothesis was rejected, and the two groups were shown to be significantly different. The effector created a significant increase in the percentage of microparticle spacers to bacteria. Overall, such a high percentage of binding, 84.8%, for the microparticle spacer with effector proved that this spacer effectively binds to bacteria.

For the computational method and visual method comparison, the percent difference resulted in 13.3%. This percent difference is relatively high. The visual method is assumed to be accurate due to human error being the only source of error; therefore, the computational method needs to be further altered to be more precise and accurate.

Error, Limitation, and Unexpected Results

One possible error is that the number of microparticle spacers used in each trial may have been inconsistent. To minimize this error, the microparticle spacers were mixed in the DNA annealing buffer using a mixer every time before extraction for data collection. This mixing prevented the spacers from collecting at the bottom of the buffer and made the concentration of spacers more consistent throughout the buffer. Also, when collecting for imaging, the spacers were always extracted from the center of the PCR tube to try to keep concentration consistent.

The computational method has many potential sources of error. Possible errors with the computational method are too small boundaries being identified around the spacers and the code incorrectly recognizing color regions, preventing some bacteria and spacers from being counted. The poor resolution of some of the images made it hard for some of the images to be analyzed; some spacers did not appear red, so they were not counted by the code.

One limitation of this study was the sample size of the data. Since the data was analyzed visually and then compared to the computational method, the number of images that could be analyzed by hand was limited due to the length of time it takes a human to analyze each image. Once the computational method is reliable enough to be used as the sole analysis method, the number of images that can be studied will increase. This will improve reliability by producing a greater sample size.

Future Work

Moving forward, the microparticle spacer will be implemented in bacterial biofilms to test for eradication levels. To test its effect, spacers will be added to the biofilms through cholesterol binding, and then, antibiotics, such as ampicillin and gentamicin, will be ran through. The percentage of bacteria in the biofilm before and after the application of antibiotics will be compared for both biofilms containing spacers and biofilms not containing spacers. Due to the spacer's demonstrated high binding affinity, we hypothesize that a high percentage of bacteria will be eradicated in the biofilms containing microparticle spacers.

The computational method will continue to be edited to improve precision and accuracy. Images with higher concentrations of bacteria and spacers will be tested to determine the effect of particle concentration on the code's accuracy. During eradication testing, the code will be used with images taken over a period of time, so the computational time per image will need to be minimized so a higher number of images does not take an exceedingly long period of time to analyze.

If eradication testing is successful, the microparticle spacer design may be changed to include a protein that can bind to the surface of specific bacteria instead of a cholesterol. Using a protein would allow for higher specification, which is needed before this design could be implemented in real life scenarios.

CHAPTER 5

CONCLUSION

Bacterial biofilms are tightly packed regions of bacteria that are difficult to treat with antibiotics due to their density and increased tolerance to antibiotics. Our microparticle spacer can successfully attach to 84.8% of the bacteria in the biofilms and decrease the tolerance of these biofilms, allowing them to be eradicated more easily. Compared to other methods of biofilm prevention and dispersion, our method is more innovative and potentially more successful at eradicating biofilms depending on the results of our oncoming eradication studies. Along with use for biofilm eradication, our microparticle spacer may also be used in diagnostic and therapeutic technology. To test its diagnostic or therapeutic properties, a Dynabead MPC-S magnetic particle concentrator could be used with the microparticle spacers. Since the Dynabeads are magnetic, the MPC-S could use magnetic force to accumulate all the microparticle spacers to one region, and this desired region containing the microparticle spacers could be removed from the rest of the sample. Since these spacers would be attached to bacteria, this accumulation could allow a larger percentage of bacteria to be analyzed at once, making it easier to diagnose the microbe and bacterial infection. This method of accumulating bacteria, or possibly viruses, could also make it easier to remove blood-borne illnesses from blood during dialysis. Once eradication studies have been completed and the microparticle spacer's success is determined relative to current work in the field, the microparticle spacer may be tested for diagnostic and therapeutic properties as well.

REFERENCES

1. Petrova, O. E., & Sauer, K. (2012). Sticky Situations: Key Components That Control Bacterial Surface Attachment. *Journal of Bacteriology, 194*(10), 2413-2425. doi:10.1128/jb.00003-12

2. Joo, H.-S., & Otto, M. (2012). Molecular basis of in-vivo biofilm formation by bacterial pathogens. *Chemistry & Biology, 19*(12), 1503-1513. doi:10.1016/j.chembiol.2012.10.022

3. Macfarlane, S., & Dillon, J. F. (2007). Microbial biofilms in the human gastrointestinal tract. *J Appl Microbiol, 102*(5), 1187-1196. doi:10.1111/j.1365-2672.2007.03287.x

4. Narisawa, N., Haruta, S., Arai, H., Ishii, M., & Igarashi, Y. (2008). Coexistence of Antibiotic-Producing and Antibiotic-Sensitive Bacteria in Biofilms Is Mediated by Resistant Bacteria. *Appl Environ Microbiol, 74*(12), 3887. doi: 10.1128/aem.02497-07

5. Hunt, S. M., Werner, E. M., Huang, B., Hamilton, M. A., & Stewart, P. S. (2004). Hypothesis for the role of nutrient starvation in biofilm detachment. *Appl Environ Microbiol, 70*(12), 7418-7425. doi:10.1128/aem.70.12.7418-7425.2004

6. Applegate, D. H., & Bryers, J. D. (1991). Effects of carbon and oxygen limitations and calcium concentrations on biofilm removal processes. *Biotechnol Bioeng, 37*(1), 17-25. doi:10.1002/bit.260370105

7. Hall-Stoodley, L., Costerton, J. W., & Stoodley, P. (2004). Bacterial biofilms: from the

natural environment to infectious diseases. *Nat Rev Microbiol, 2*(2), 95-108. doi:10.1038/nrmicro821

8. Cheng, G., Xite, H., Zhang, Z., Chen, S. F., & Jiang, S. Y. (2008). A switchable biocompatible polymer surface with self-sterilizing and nonfouling capabilities. *Angewandte Chemie-International Edition, 47*(46), 8831-8834. doi:10.1002/anie.200803570
9. Shahrooei, M., Hira, V., Stijlemans, B., Merckx, R., Hermans, P. W., & Van Eldere, J. (2009). Inhibition of Staphylococcus epidermidis biofilm formation by rabbit polyclonal antibodies against the SesC protein. *Infect Immun, 77*(9), 3670-3678. doi:10.1128/iai.01464-08
10. Prateeksha, Singh, B. R., Shoeb, M., Sharma, S., Naqvi, A. H., Gupta, V. K., & Singh, B. N. (2017). Scaffold of Selenium Nanovectors and Honey Phytochemicals for Inhibition of Pseudomonas aeruginosa Quorum Sensing and Biofilm Formation. *Frontiers in Cellular and Infection Microbiology, 7*, 93. doi:10.3389/fcimb.2017.00093